Automatic Image-To-Map-Registration of Remote Sensing Data

HEINER HILD, Stuttgart

ABSTRACT

With this paper, a fully automatic system for the registration of satellite image data with vector GIS data is presented. The implemented approach is based on polygonal objects which are extracted from the image (region growing segmentation) and from the GIS data set (merging of polygons with the same object class). Based on absolute affine invariant features, corresponding pairs of objects are determined by a backtracking depth-first tree search algorithm. Investigations concerning the robustness and discrimination power of the used absolute affine invariants are presented. Within the tree search algorithm, unary and binary constraints are applied in order to find a consistent subset of polygon pairs from all matching hypothesis. Furthermore, a coarse global affine transformation is determined in this step. Based on this transformation, all hypothesis being consistent with the global transformation are determined in a verification step. An individual affine transformation for each object pair is computed by using the formalism of standard positions., The individual transformations are refined for each verified sensor-model polygon pair in a refinement step. Finally, homologuous points (GCPs) with prefixed standard deviation of the residuals are extracted from the polygon boundaries. The whole process is exemplarily applied to a 25km x 20km section of the German ATKIS Vector data base and corresponding original SPOT PAN data. In this work, only forest polygons were used.

1. INTRODUCTION

The still growing number of remote sensing imagery raises the need of a reliable automatic system to solve the georeferencing problem. Integration of GPS and INS measurements to determine the exterior orientation becomes an operational strategy for airborne imaging systems (Cramer, 2000), GPS/INS and star tracker measurements are also becoming standard for space borne systems. However, in operational processes, satellite images are up to now mainly georeferenced by manual measurements. Based on image-to-image registration techniques (Fonseca & Manjunath, 1996), several systems have been proposed to solve the problem of georeferencing satellite images, e.g. the ARCHANGEL project (Dowman, 1998), (Dowman & Ruskoné, 1997), (Hild & Fritsch, 1998). The ARCHANGEL system relies on polygonal patches of satellite and raster GIS data, using chain code frequencies of the patch boundaries (Abbasi-Dezfouli & Freeman, 1994). Satellite image objects are computed by region growing segmentation. Following the basic idea of matching area objects between satellite images and GIS data, Sester et al. (1998) proposed a system where a coarse-to-fine strategy is applied. In this work, forest objects in the satellite image were extracted by multispectral classification. Matching object pairs are generated by the use of unary and binary constraints in a constrained tree search process (Grimson, 1990), followed by a verification step which leads to a global affine transformation between sensor and GIS data. Transformation refinement is achieved by using the Iterative Closest Point (ICP) algorithm (Besl & McKay, 1992). Another system which also uses area objects to register images with images and images with maps was proposed by Holm et al. (1995). Where the ARCHANGEL system needs the image scale as prerequisite information, Holm et al. (1995) use invariant moments – besides others – as features for the objects. Hereby, ideas of computer vision were merged with the georeferencing task. Invariants from geometric moments were introduced by Hu (1962) and have been widely used since then for various pattern recognition and shape discrimination works (Flusser & Suk, 1993), (Abu-Mostafa & Psaltis, 1984), (Chen, 1993). A comprehensive overview on image analysis by moments is given by Teh (1988). The work for this paper is based on ARCHANGEL and integrates affine invariant features of polygonal objects into an improved and further developed system from Sester et al. (1998). The focus for solving the georeferencing problem in a fully automatic way was set on independence of

thresholds, approximate values and manual interactions. The only necessary assumption is, that satellite image data and GIS data can be approximately transformed onto each other by an affine transformation. Studies of the author not presented here have proven the legacy of this assumption for practically occurring cases. The paper outlines in detail the single steps which were implemented and successfully tested.

2. OBJECT GENERATION

The basic concept of this work consists of matching area objects from satellite images and GIS data sets based on invariant features. No prior information about image scale or sensor orientation shall be used. On the satellite image hand, an adaptive threshold segmentation algorithm was chosen from the numerous already developed segmentation algorithms to generate area objects with certain gray value homogeneities (Levin & Shaheen, 1981). The selected algorithm performs a region growing, using an adaptive threshold instead of a fixed one. Let N be the actual number of pixels in the actual region R_i, the gray value of a pixel in row r and column c may be $g(r,c)$. Then, the relevant statistical values of the region R_i compute to:

$$\text{Mean gray value of the region:} \quad M_{R_i} = \frac{1}{N} \sum_{(r,c)\in R_i} g(r,c) \tag{2.1}$$

$$\text{Standard deviation of the region:} \quad \sigma_{R_i} = \frac{1}{N} \left[\sum_{(r,c)\in R_i} \left[g(r,c) - M_{R_i} \right]^2 \right]^{1/2} \tag{2.2}$$

Since the interesting objects are located in the foreground, a 4-neighborhood relation is applied to grow a region R_i. A pixel in the 4-neighborhood of the actual pixel is assigned to the region if $|g_n(r_n,c_n) - g(r,c)| < AT$ (adaptive threshold), where (r_n,c_n) are the 4-neighbors of (r,c) and $g_n(r_n,c_n)$ is the corresponding gray value.

The adaptive threshold AT computes from the region statistics and the user defined fixed threshold T to:

$$AT = \left[1 - \min(0.8, \frac{\sigma'_{R_i}}{M'_{R_i}}) \right] \times T, \tag{2.3}$$

where σ'_{R_i} and M'_{R_i} include the actual pixel.

The dynamically modified adaptive threshold AT cannot exceed the fixed threshold T but can become much smaller. Adaptive thresholding is useful e.g. in preventing bleeding across smooth image gradients. In Figure 2.1, the effect of various fixed thresholds on the adaptive threshold segmentation is illustrated with a section of a SPOT PAN scene.

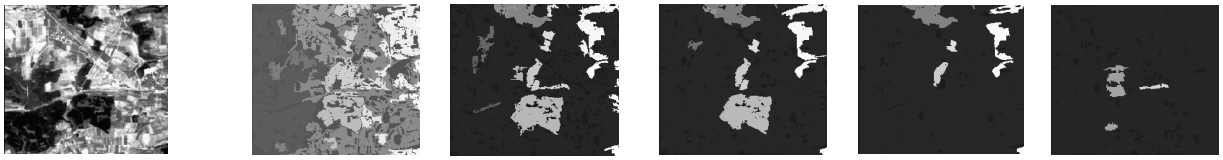

Histogram stretched image section | AT=3 | AT=5 | AT=7 | AT=10 | AT=15

Figure 2.1: Influence of fixed threshold values on adaptive threshold region growing segmentation of SPOT PAN data

As can be seen clearly, the results are ranging from oversegmentation (AT=3) to undersegmentation (AT=15). The assumption in this step is, that within a parameter range, most of the relevant objects

are segmented correctly. Hence, the correct segmentation results will be included in the whole set of segmented objects.
Due to the specific rules of capturing data for a certain GIS database, the GIS area objects do not necessarily represent complete units of a given class. Forest patterns, e.g., are sometimes separated by small paths which normally are not visible in a satellite image. Therefore, area objects are taken from the attributed ATKIS data set and adjacent objects of the same class are simply merged in a standard GIS package (Arc/View) in order to obtain aggregated objects which can be identified in the satellite scene. In this work, holes of polygons are not considered for segmentation results as well as for merged GIS objects. ATKIS forest objects of a 25km x 20km area are given with Figure 2.2; the merged result is shown in Figure 2.3.

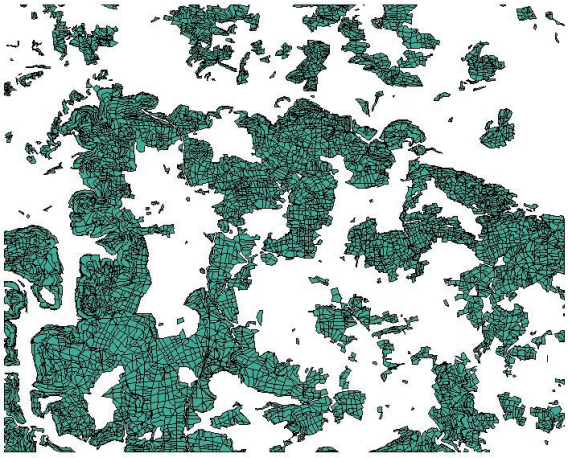

Figure 2.2: ATKIS forest polygons in 25km x 20km test area.

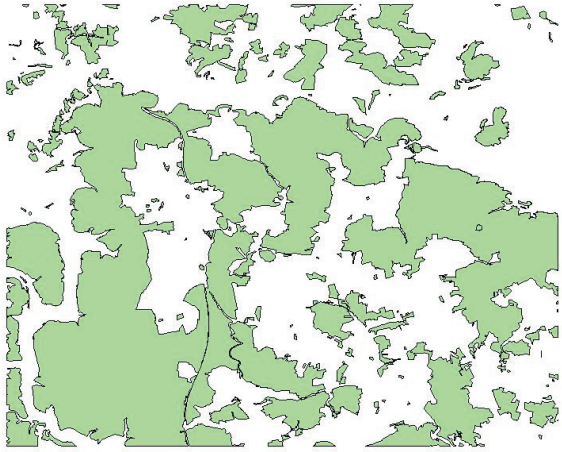

Figure 2.3: Merged ATKIS forest polygons as input for automatic GCP location.

3. EXTRACTION OF AFFINE INVARIANT FEATURES

The prerequisite for matching sensor and map data without any prior information about sensor orientation, projection center location or image scale is an object description which is invariant under an allowed type of transformation, namely an affine transformation for this work. Area objects are chosen to be the basic objects to be used for automatically establishing the georeference of sensor imagery. Hence, the problem to be solved is to extract affine invariant features of polygons, which can be computed in vector and raster domain simultaneously. In computer vision, affine invariants based on geometric moments were first introduced by Hu (1962). The computation of geometric moments is depicted with Figure 3.1.

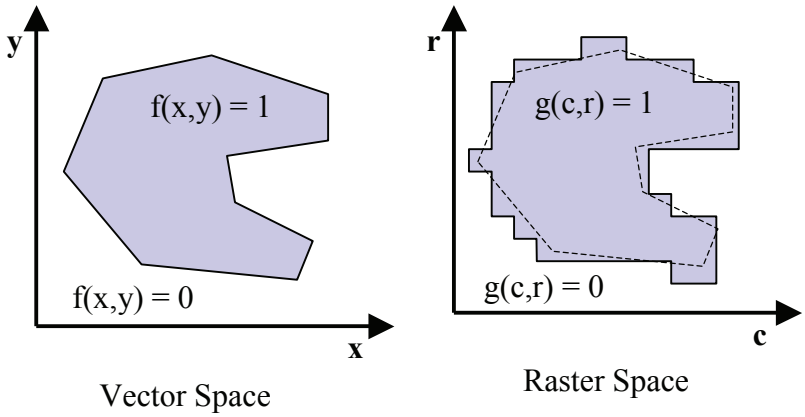

Figure 3.1: Area objects in Raster and vector space.

In this context, area objects are described by a function *f(x,y)* rsp. *g(c,r),* which is 1 inside and 0 outside the object. Given the object's center of mass by $(\bar{x},\bar{y})$ rsp. $(\bar{c},\bar{r})$, central geometric

moments of order *(p+q)* for vector objects are defined as:

$$m_{pq} = \iint (x-\bar{x})^p (y-\bar{y})^q f(x,y)dxdy\,, \tag{3.1}$$

where the corresponding definition for raster objects looks like:

$$m_{pq} = \sum_{r,c} (c-\bar{c})^p (r-\bar{r})^q g(c,r)\,. \tag{3.2}$$

Since the computation of central geometric moments by integration or summation over the whole object area is relatively time consuming, faster methods of computing central geometric moments directly from the object's boundary *C(G)* were developed (Singer, 1993). Based on Green's integral theorem

$$\iint_G \left(\frac{\partial u}{\partial x} - \frac{\partial v}{\partial y}\right) dxdy = \oint_{C(G)} (udy + vdx)\,, \tag{3.3}$$

the integral to be solved can be written as:

$$m_{pq} = \oint_{C(G)} \frac{(x-\bar{x})^{p+1}}{p+1} y^q dy\,. \tag{3.4}$$

How can central geometric moments be used for the generation of affine invariant features?

Yang & Cohen (1999) proposed a procedure where so-called cross weighted moments (CWMs) are used to generate absolute affine invariants. The CWMs can be expressed in terms of central geometric moments, leading to the following absolute affine invariants:

$$\Phi(s_0,s_1) = \frac{\sqrt[s_1+2]{\sum_{g_1=0}^{s_1} (-1)^{s_1-g_1} \binom{s_1}{g_1} m_{g_1,s_1-g_1} m_{s_1-g_1,g_1}}}{\sqrt[s_0+2]{\sum_{g_0=0}^{s_0} (-1)^{s_0-g_0} \binom{s_0}{g_0} m_{g_0,s_0-g_0} m_{s_0-g_0,g_0}}}\,. \tag{3.5}$$

When central geometric moments are used, s_0 and s_1 must be positive, even integers and $s_1 > s_0$ must hold true, e.g. (4,6) or (4,8) etc. In clear words, the properties $\phi(s_0,s_1)$ can be directly computed from a polygonal object boundary and do not change their specific values when the

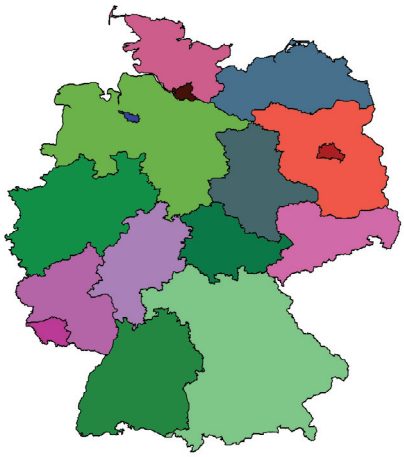

Figure 3.2: The federal states of Germany as test objects.

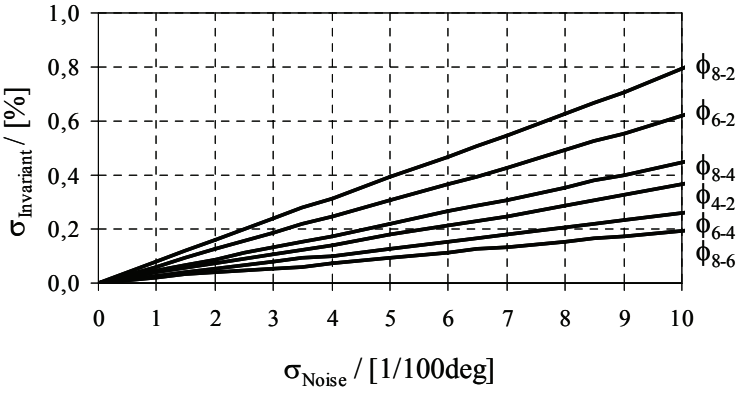

Figure 3.3: Influence of random noise on the standard deviation of various absolute affine invariants of German state boundaries.

object is transformed with an arbitrary affine transformation, i.e. any rotation, shearing, translation or mirror operation.

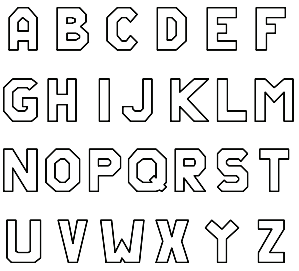

Figure 3.4: Vector letters test data set.

The expressions of eqn. (3.5) are absolute invariants for any exactly affine copy of a certain area object. In real object pairs, however, this situation is very unlike due to non-affine transformations, changes in the objects, distortions from topography or digitization and the like. For these reasons, the behavior of absolute affine invariants $\phi(s_0,s_1)$ was studied under various effects. In Figure 3.3, the influence of random noise in x and y is shown for the boundaries of the federal states of Germany, illustrated with Figure 3.2. The standard deviation of the applied artificial x,y-noise ranged from 0deg to 0.01deg (~1000m). As can be seen clearly, the normalized standard deviation of all invariants is lower than 1%, i.e. a high robustness against random noise could be stated[1].

Invariance of features under a given transformation is only one aspect for successfully matching polygonal objects. Another criteria, which must be fulfilled by a reasonable choice of features, is their potential to discriminate different objects. However, an ideal set of features would be robust under transformations similar to the exact one and sensitive to significant shape changes. Naturally, these extremes cannot be fulfilled similarly. In order to study the discrimination potential of the $\phi(s_0,s_1)$, another experiment was carried out. For the boundaries of vector letters, shown in Figure 3.4, the appearance in a segmented raster image was simulated by using various raster sizes. This setup allows to study the matching and discrimination potential of affine invariants in an analytical way. In Figure 3.5, the letter "K" is exemplarily shown in various raster sizes. For a certain level of generalization, the letter pairs with minimal euclidian distance in the 6D feature space formed by the six most simple affine invariants $\{\phi(4,2),\phi(6,2),\phi(8,2),\phi(6,4),\phi(8,4),\phi(8,6)\}$ were determined.

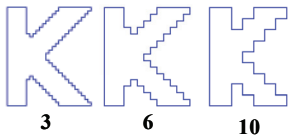

Figure 3.5: The letter "K" in different raster widths.

The result is shown in Figure 3.6. Both mapping directions (original → generalized and generalized → original) were examined for each raster size.

Concluding this section, it can be stated that absolute affine invariants based on Cross-Weighted Moments are suitable properties for matching area objects of satellite image on the one hand and GIS data sets on the other hand. Although not all extracted objects can be discriminated and matched correctly, however, the rate of correct results is sufficient since with the further strategy only a few correct matches are necessary in order to establish an approximate affine transformation between satellite image and GIS data set.

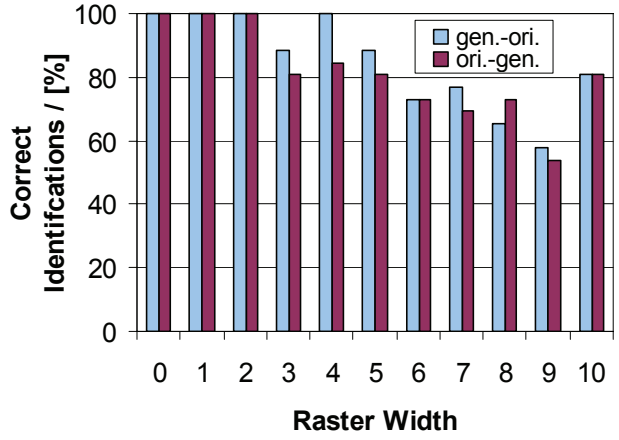

Figure 3.6: Correct Letter identifications based on minimal feature space distance for pairs of vector and raster letters.

[1] Absolute affine invariants based on algebraic invariants, as they are frequently used for pattern recogntion, are less robust under the influence of noise (Abu-Mostafa & Psaltis, 1984), (Teh, 1988).

4. MATCHING AND VERIFICATION

The objective of the matching and verification step is the determination of a consistent set of sensor-model object pairs. For this work, a depth-first backtracking tree search strategy, using unary and binary constraints was implemented (Grimson, 1990). In this context, a consistent number of sensor-model pairs are given when all constraints are fulfilled simultaneously. In conventional processes, only one set of sensor features is subjected to the search. Within this work, several segmentation runs are performed with different thresholds and all objects from each run are considered as match candidates for each model data set object M_i. The backtracking tree search starts at the root and subsequently checks the nodes of the next level for consistency by evaluating the constraints. When a node is consistent, it is added to the current set and the next level of the tree is inspected. Once an inconsistency is found or no further node is available on the current level, a backtracking step takes place where the last node in the current interpretation is removed (since it is not expandable any more) and the next branch in the higher level is inspected. When a leaf of the tree is reached (i.e. a sensor object for M_k is found), the whole set is saved as a consistent interpretation. In order to avoid search breakdown when no real sensor object can be found for a certain model object M_i, virtual matches are allowed for each tree level where a wildcard sensor element is assigned to M_i. The constraints applied in the search process are in detail:

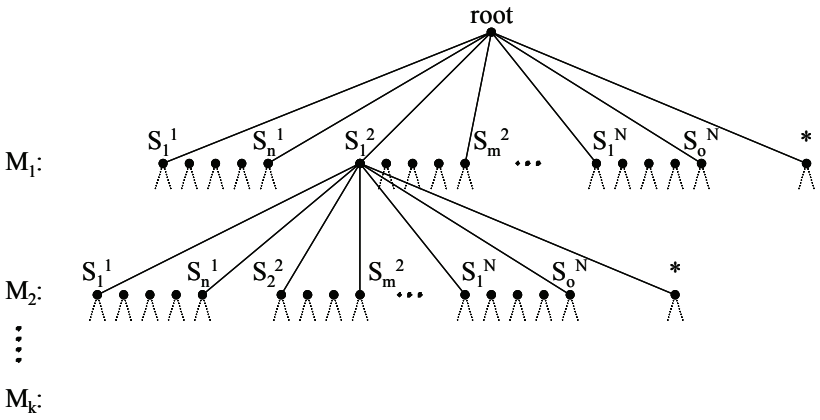

Figure 4.1: Search tree for N segmentation runs $S^{1,\ldots,}S^N$ with wildcard elements to prevent breakdown of the search.

Area (unary): Only sensor objects with a certain size relative to the image size are subjected to the tree search (e.g. bigger than 1 / 10 000 of the image size).

Invariant Space Distance (unary): The normalized distance in 6D feature space formed by the 6 absolute affine invariants, which were given in the last section, must not exceed a certain value (e.g. 5% of the smaller vector norm).

Centroid Transformation (binary): The minimum bounding rectangle (MBR), which touches the object and has minimum area, is computed for each sensor and model object. The transformed object centroids of two object pairs must mutually be located inside the partner's MBR. The transformation is taken from the partner object pair respectively. The determination of the individual affine back and forth transformations for each pair is described below.

Form (binary): The polygons of an object pair, transformed with the transformation parameters of the second pair, must overlap for more than a certain percentage (e.g. 75%). This check is also performed mutually. This is the most restrictive but also the most expensive constraint, therefore it is evaluated last.

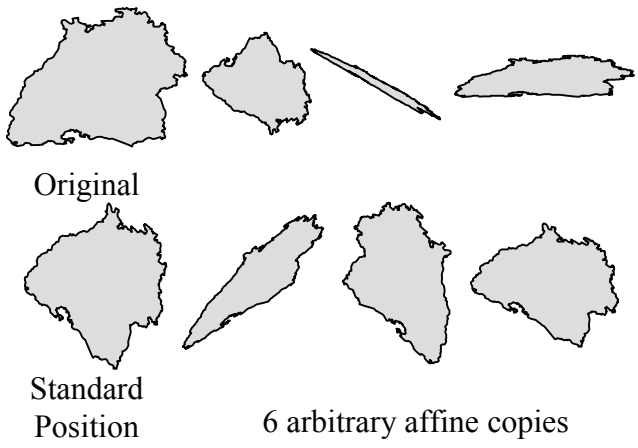

Figure 4.2: The boundary of Baden-Württemberg, six arbitrary affine copies and their common standard position.

In order to decrease the computational effort for the tree search, several extensions are applied. The search must not necessarily reach a leaf of the tree but breaks down when a certain depth (e.g. 5) is reached. Therefore, a heuristic can be applied by sorting the object pairs by the products of their areas, i.e. big-big pairs are inspected earlier than small-small pairs. Since the main goal of the work is the derivation of GCPs which shall best be distributed widely over the scene, this heuristic leads to best spread objects and hence possible GCPs on their boundaries. Applying unary constraints before the search is started, implies another simplification: multiple computations of the same constraints are avoided. Pre-classifying the pairs before the feature space constraint is checked reduces the computational effort again. When the desired depth of the search tree is reached, the actual set of consistent scene-model object pairs is stored and an approximate global affine transformation is computed by weighted averaging of the back and forth transformation parameters of each pair of the set. The weights are taken from the inverse normalized euclidian distance in the 6D-space which is spanned by the absolute affine invariant features described above.

It has already been pointed out that the affine back and forth transformation between hypothetically matching objects is needed during the search process in order to evaluate various constraints. In earlier works (Sester et al., 1988), the transformations have been computed from the corresponding MBR corners. Since central geometric moments were already computed, a more elegant and even more accurate procedure can be exploited. By scaling certain moments, a so-called standard position can be computed for each object, which is unique for all possible affine transformations, including mirror operations. Different strategies for computing the standard position of 2D polygons are described in Süße (1999). For this work, the iterative strategy was implemented, since it is the most robust one. When the standard position is computed, possible x- and y-shear is removed first by iteratively shearing the object in x- and y-direction until the moments m_{31} and m_{13} are vanishing simultaneously. In the next phase, x- and y-scaling operations are performed in order to scale m_{20} and m_{02} to the same constant value for all objects (here: 10 000 square units). Finally, the ambiguity for rotations by multiples of 90° and for mirror operations is removed by ensuring $m_{21} > m_{12} > 0$. The transformation into the standard position is determined then by combining all applied transformations. Let the standard transformation for object O_i be $T_i(O_i)$. Then, the transformation from O_i to O_j computes to:

$$T_{i\to j}(O_i,O_j) = T_i^{-1}(O_i) * T_j(O_j) \tag{4.1}$$

and vice versa.

Due to the use of affine invariant features and their robustness against perturbations, the whole process of determining a global affine transformation between GIS and sensor data is very robust. In order to illustrate the robustness, an ATKIS data set was undertaken several transformations before being subjected to the matching process. As can be seen in Figure 4.3, the obtained coarse transformation is acceptable in each case.

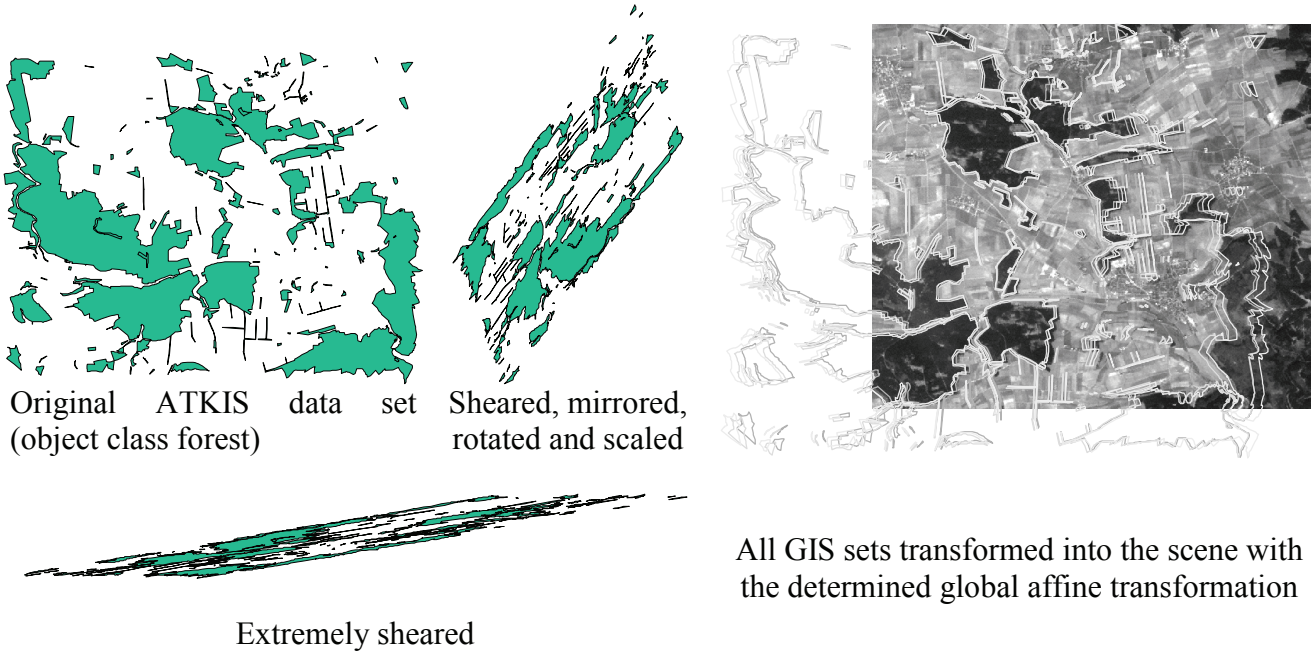

Figure 4.3: Examples for the robustness of the fully automatic determination of a global affine transformation between ATKIS GIS data and a section of a SPOT PAN scene.

In the set of hypothetically matching pairs there are numerous wrong matches besides the correct ones. A verification step, based on the already existing coarse global back and forth affine transformation, is applied in order to extract only the correct matches from this set. In the first step of the verification process, the back and forth transformation for each pair is converted from six matrix elements into rotation angles, scale factors and translations for the x- and the y-axis. A rough selection of wrong pairs is applied by eliminating all hypotheses where at least one of these six parameters exceeds a limited range around the corresponding parameter of the global transformation. Even with relatively coarse selection thresholds (angles: ±45°, relative scales and translations: ±70%) most of the wrong hypothesis can be eliminated with this strategy. In a second step, it is ensured that each of the model and sensor objects is occurring only once in the verified hypothesis data set. If there are multiple occurrences, the relative overlap for all pairs containing a multiply occurring object is computed and the pair with the largest overlap is kept while the rest is eliminated.

5. GCP GENERATION AND RESULTS

So far, verified sensor-model polygon pairs are computed with an individual back and forth affine transformation. When an approximate transformation is given, a computer vision algorithm for precisely registering two geometric objects in 2D or 3D can be applied as proposed by Besl & McKay (1992): The Iterative Closest Point algorithm (ICP). Without going in too many details, the basic idea of this algorithm is iteratively improving a given object-to-object transformation by selecting points on one object boundary (or surface), determining the closest point of the partner boundary (or surface) and re-estimating the desired type of transformation from this set of closest-distance point pairs. If no significant improvement of the transformation can be achieved, the algorithm breaks down. The collection of closest points is carried out over all verified polygon pairs before the transformation estimation is taking place. For this work, the ICP algorithm was extended in some way: A new point pair is only accepted during one iteration if its distance does not exceed a certain but fixed percentage of the standard deviation of all point pairs. With this extension, partly correct correspondences can also be handled, which would have been impossible with the standard

ICP algorithm. Furthermore, an affine and a projective transformation is estimated for each pair. The transformation leading to the lower standard deviation of the accepted point pair distances is finally considered as best possible refined individual object-object match.

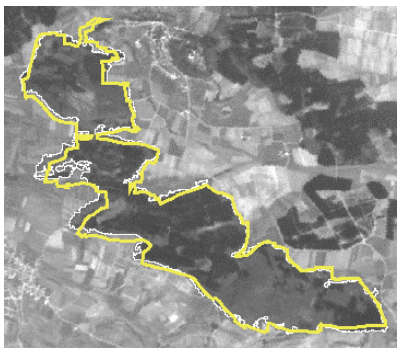

Figure 5.1: Segmentation result (thin line) and transformed GIS polygon (thick line) using the standard position only.

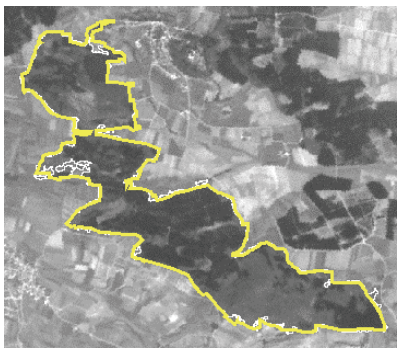

Figure 5.2: Segmentation result (thin line) and transformed GIS polygon (thick line) modified after ICP refinement.

Once the refined sensor-model object transformation is computed, theoretically an infinite number of homologue point pairs (GCPs) could be generated. However, practically useful GCPs should fulfill certain criteria, like distinctness, ease of identification and equal spread over the whole scene, just to name a few. Within this work, all vertices of the verified GIS polygons are taken as possible GCPs. In order to get reliable points, a selection is applied, where only polygon vertices with face intersection angles larger than a certain value (e.g. 45°) are chosen. This procedure ensures that GCPs are located on corners and not on a straight line. In order to get the best points out of this still big set of points, all selected GCPs are first sorted by their residuals. Beginning from the point pair with the lowest residual, either a defined number of pairs is taken or the points are accepted until a defined standard deviation (e.g. 0.2pix) is reached. By individually setting the minimum angle at each vertex and the maximum standard deviation or number of final GCPs, the focus can be set either on higher accuracy (bigger minimum angle and smaller standard deviation) or on bigger number (smaller minimum angle, bigger standard deviation). In Figure 5.4, an example is given for a 25km x 20km area in southern Germany. GCPs were taken from the GIS data set. The minimum angle at each vertex was set to 45° where the maximum standard deviation of the obtained GCPs is 0.2pix i.e. 2m for the SPOT PAN scene. There are overall 6084 GCP polygon vertices in the data set with

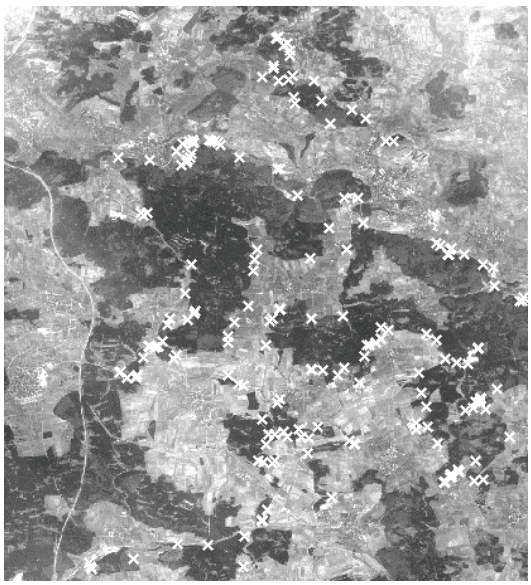

Figure 5.3: SPOT test area with automatically detected GCPs.

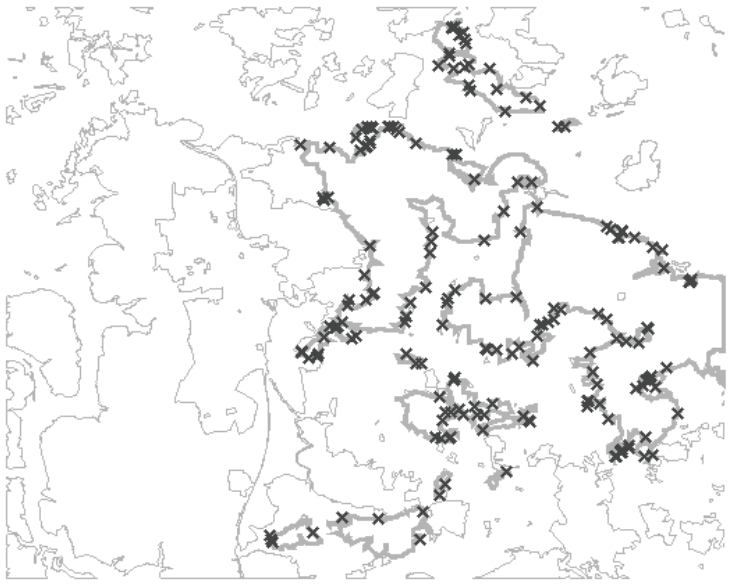

Figure 5.4: German ATKIS GIS test data set (thin line) with automatically detected GCPs on verified GIS polygons (thick line).

a standard deviation of the residuals of 94.1m. With the already presented settings, the whole GCP generation process resulted in 190 GCPs (with a standard deviation of 2m), well spread all over the scene (Figure 5.3)

6. CONCLUSION

Within this work, a system is presented, which generates GCPs in a fully automatic way. The presented system needs no approximate values, neither for the image scale nor for the sensor orientation, since features which are absolutely invariant under affine transformation are used. The only prerequisites for a successful run are: The remote sensing scene and the GIS data set must contain identical objects and an affine transformation is principally applicable for a coarse georeference. The proposed approach is based on polygonal features from both data sets. First, relevant objects are extracted and six invariant features based on Cross Weighted Moments (CWM) are computed. A possibility, how CWMs can be computed from the geometric moments and hence directly from the object boundary is outlined. In the matching step, all possible corresponding object pairs are determined. Possible candidates are characterized by distances in 6D feature space which are smaller than a certain threshold. A consistent subset is determined from all hypothetic pairs by applying a constraint tree search. The search strategy is a depth-first backtracking tree search with virtual matches. From the consistent subset, a global back and forth affine transformation is computed, transforming GIS data and sensor data coarsely into each other. An individual affine transformation is computed for each matching pair using the formalism of standard position in an iterative approach. With the global affine transformation and the individual transformation, a verification step is taking place which separates correct from erroneous matches. The verified polygon pairs are undertaken a refinement of the individual transformation. In this step, a modified version of the Iterative Closest Point (ICP) algorithm, well known in computer vision, is applied. Finally, GCPs are extracted from the refined polygon pairs. The implemented system allows for choosing either more or better GCPs, in any case only point pairs from the polygon boundaries with low residuals are selected. In a presented example of a 25km x 20km test area, 190 GCPs with a standard deviation of 2m (20% of the SPOT PAN GSD) of the residuals were generated from overall 216 merged forest GIS data polygons with overall 6084 vertices. The presented approach works in a fully automatic way and is very robust due to several factors:

- A number of segmentation runs is performed automatically in order to generate sensor data set objects. With this strategy, independence from radiometric variances can be obtained.
- Absolute affine invariants are used for the matching process.
- Presented studies showed that invariant features are robust under noise but on the same hand have enough potential to discriminate objects with different shapes.
- A coarse to fine strategy is applied.

7. REFERENCES

Abbasi-Dezfouli, M.; Freeman, T. (1994): Patch Matching in Stereo-Images Based on Shape, in: Spatial Information from Digital Photogrammetry and Computer Vision, Eds. H. Ebner, C. Heipke, K. Eder, München, pp. 1-8

Abu-Mostafa, Y.; Psaltis, D. (1984): Recognitive Aspects of moment invariants, IEEE Trans. PAMI, Vol.6, pp. 698-706

Besl, P. J.; McKay, N. D. (1992): A method for Registration of 3-D Shapes, IEEE Trans. PAMI, Vol.14(2), pp. 239-256

Chen, C.-C. (1993): Improved Moment Invariants for Shape Discrimination, Pattern Recognition, Vol.26(5), pp. 683-686

Dowman, I. (1998): Automatic Image Registration and Absolute Orientation: Solutions and Problems, Photogrammetric Record, Vol. 16(91), pp. 5-18

Dowman, I.; Ruskoné, R. (1997): Extraction of Polygonal Features from Satellite Images for Automatic Registration: The ARCHANGEL Project, in: Automatic Extraction of Man Made Objects from Aerial and Space Image, Birkhäuser Verlag, pp. 343-354

Cramer, M. (2000): Genauigkeitsuntersuchungen zur GPS/INS-Integration in der Aerophotogrammetrie, Dissertation, Universität Stuttgart

Flusser, J.; Suk, T. (1993): Pattern Recognition by Affine Moment Invariants, Pattern Recognition, Vol.26, pp. 167-174

Fonseca, L. M. G.; Manjunath (1996): Registration Techniques for Multisensor Remotely Sensed Imagery, Photogrammetric Engineering & Remote Sensing, Vol. 62(9), pp. 1049-1056

Grimson, W. E. L. (1990): Object Recognition by Computer: The Role of Geometric Constraints, MIT Press, Cambridge, Mass.

Hild, H.; Fritsch, D. (1998): Integration of Vector Data and Satellite Imagery for Geocoding, ISPRS Comm. IV Symposium: GIS-Between Visions and Applications, Eds. D. Fritsch, M. Englich; M. Sester, , Stuttgart, pp. 246-251

Holm, M; Parmes, E.; Andersson, K.; Vuorela, A. (1995): A nationwide automatic satellite image registration system, SPIE Aerosense '95 - Conference on Integrating Photogrammetric Techniques with Scene Analysis & Machine Vision II, Orlando, Florida, USA, pp. 156-167

Hu, M. K. (1962): Visual pattern recognition by moment invariants, IEEE Transactions on Information Theory, Vol.8, pp. 179-187

Levine, M. D.; Shaheen, S. I. (1981): A Modular Computer Vision System for Picture Segmentation and Interpretation, IEEE Trans. PAMI, IEEE Trans. PAMI, Vol.3(5), pp. 540-556

Sester, M.; Hild, H.; Fritsch, D. (1998): Definition of Ground-Control Features for Image Registration using GIS-Data, ISPRS Comm.III Symposium on Object Recognition and Scene Classification from Multispectral and Multisensor Pixels, IAPRS, Vol.32/2, Eds. Schenk, T & Habib ,A., Columbus/Ohio, USA, pp. 537-543

Singer, M. H. (1993): A General Approach to Moment Calculation for Polygons and Line Segments, Pattern Recognition, Vol.26(7), pp. 1019-1028

Teh, C. -H.; Chin, R. T. (1988): On Image Analysis by the method of moments, IEEE Trans. PAMI, Vol.10(4), pp. 496-513

Süße, H., Tutorium Bildanalyse mittels Invarianten, 21. DAGM-Symposium für Musterekennung, DAGM, Bonn, pp. 1-93

Yang, Z.; Cohen, F. S (1999): Cross-Weighted Moments and Affine Invariants for Image Registration and Matching, IEEE Trans. PAMI, 804-814, Vol.21(8), pp. 804-814